

Phase sensitive sensor on plasmonic nanograting structures.

M. Maisonneuve, O. d'Allivy Kelly, A-P. Blanchard-Dionne, S. Patskovsky, and M. Meunier

Laser Processing and Plasmonics Laboratory, Department of engineering physics, École Polytechnique de Montreal, Montréal, Québec Canada

Abstract: In this paper, a concept of phase sensitive sensor based on plasmonic nanograting structures with normal incidence and transmission detection is presented. Performed theoretical modeling enables fabrication of nanostructures with optimal geometry for polarimetric measurements of the phase difference between s- and p- polarized light. High phase resolution of the optical setup (6×10^{-3} deg.) allows detection of the bulk refractive index with sensitivity equal to 3.8×10^{-6} RIU. Proposed technique presents a more efficient alternative to the conventional spectral interrogation method of nanoplasmonic-based sensing and could be used for multisensing or imaging applications.

OCIS codes: (120.5050) Phase measurements; (240.6680) Surface plasmons; (050.2770) Gratings.

References and Links

1. F. J. Garcia-Vidal, T. W. Ebbesen, and L. Kuipers, "Light passing through subwavelength apertures," *Rev. Mod. Phys.* **82**(1), 729–787 (2010).
2. L. Guyot, A. P. Blanchard-Dionne, S. Patskovsky, and M. Meunier, "Integrated silicon-based nanoplasmonic sensor," *Opt. Express* **19**(10), 9962–9967 (2011).
3. K. A. Willets and R. P. Van Duyne, "Localized surface plasmon resonance spectroscopy and sensing," *Annu. Rev. Phys. Chem.* **58**(1), 267–297 (2007).
4. M. Vala, K. Chadt, M. Piliarik, and J. Homola, "High-performance compact SPR sensor for multi-analyte sensing," *Sens. Actuators B Chem.* **148**(2), 544–549 (2010).
5. S. Patskovsky, M. Meunier, P. N. Prasad, and A. V. Kabashin, "Self-noise-filtering phase-sensitive surface plasmon resonance biosensing," *Opt. Express* **18**(14), 14353–14358 (2010).
6. W.-C. Law, P. Markowicz, K.-T. Yong, I. Roy, A. Baev, S. Patskovsky, A. V. Kabashin, H.-P. Ho, and P. N. Prasad, "Wide dynamic range phase-sensitive surface plasmon resonance biosensor based on measuring the modulation harmonics," *Biosens. Bioelectron.* **23**(5), 627–632 (2007).
7. P. S. Vukusic, G. P. Bryan-Brown, and J. R. Sambles, "Surface plasmon resonance on gratings as a novel means for gas sensing," *Sens. Actuators B Chem.* **8**(2), 155–160 (1992).
8. M. R. Gadsdon, I. R. Hooper, and J. R. Sambles, "Optical resonances on sub-wavelength silver lamellar gratings," *Opt. Express* **16**(26), 22003–22028 (2008).
9. M. G. Moharam and T. K. Gaylord, "Rigorous coupled-wave analysis of planar-grating diffraction," *J. Opt. Soc. Am.* **71**(7), 811–818 (1981).
10. D. L. Mills, "Attenuation of surface polaritons by surface roughness," *Phys. Rev. B* **12**(10), 4036–4046 (1975).
11. L. Martín-Moreno, F. J. García-Vidal, H. J. Lezec, K. M. Pellerin, T. Thio, J. B. Pendry, and T. W. Ebbesen, "Theory of Extraordinary Optical Transmission through Subwavelength Hole Arrays," *Phys. Rev. Lett.* **86**(6), 1114–1117 (2001).
12. H. Raether, *Surface Plasmons on Smooth and Rough Surfaces and on Gratings* (Berlin, 1988).
13. F. Abeles, "Surface electromagnetic waves ellipsometry," *Surf. Sci.* **56**, 237–251 (1976).
14. K. Knop, "Rigorous diffraction theory for transmission phase gratings with deep rectangular grooves," *J. Opt. Soc. Am.* **68**(9), 1206–1210 (1978).
15. I. Pockrand, "Resonance anomalies in the light intensity reflected at silver gratings with dielectric coatings," *J. Phys. D Appl. Phys.* **9**(17), 2423–2432 (1976).
16. G. D'Aguzzo, N. Mattiucci, M. J. Bloemer, D. de Ceglia, M. A. Vincenti, and A. Alù, "Transmission resonances in plasmonic metallic gratings," *J. Opt. Soc. Am. B* **28**(2), 253–264 (2011).
17. F. García de Abajo, "Colloquium: Light scattering by particle and hole arrays," *Rev. Mod. Phys.* **79**(4), 1267–1290 (2007).
18. E. R. Peck and B. N. Khanna, "Dispersion of nitrogen," *J. Opt. Soc. Am.* **56**, 1059–1063 (1966).

1. Introduction

Plasmonics is rapidly becoming a dominant technology in the fields of novel optical devices employing new experimental capabilities of subwavelength metallic nanostructures. In combination with modern nanofabrication technologies which allows preparation of numerous regular patterns of particles, holes, or nanogratings, this technology provides opportunities to create efficient, fast and sensitive integrated multiplexed sensor systems for biological and medical research [1, 2]. Despite a number of undisputable advantages, nanoplasmonics-based sensors show sensitivity and resolution orders of magnitude lower compared to conventional SPR devices with prism or grating coupling methods where usually detection limit is about $1 \cdot 10^{-6}$ Refractive Index Units (RIU) [3, 4]. The main problem is related to the fact that localized plasmon-based biosensors use only the resonant frequency of plasmon excitation, whereas conventional SPR takes additionally advantages of the finely tuned resonant conditions of angular or spectral coupling of a photon to the surface plasmon (SP) wave.

In this article, we propose to use a phase-sensitive detection approach to biosensing based on plasmonic nanograting structures. We think that existing phase measurement methodology which was shown as very efficient for SPR optical sensing [5, 6], could be used in combination with stabilized monochromatic laser sources to further improve the sensitivity, selectivity and resolution of plasmonics-based biosensing up to the detection limit of conventional SPR and to develop novel nanoscale plasmonics complexes and architectures.

2. Basic idea and approach

Coupling photons into surface plasmons (SP) can be achieved using a grating as a coupling medium to match the photon and SP wave vectors. A grating coupler matches the wave vectors by increasing the parallel wave vector component by an amount related to the grating period. The angle θ that satisfies the SP resonant excitation condition is given by [7]:

$$\sqrt{\varepsilon_d} \frac{2\pi}{\lambda_0} \sin(\theta) + p \frac{2\pi}{\Lambda} = \frac{2\pi}{\lambda_0} \sqrt{\frac{\varepsilon_M(\lambda) \cdot \varepsilon_d(\lambda)}{\varepsilon_M(\lambda) + \varepsilon_d(\lambda)}} \quad (1)$$

where p is an integer relative to the diffraction order, Λ is the grating period, and ε_d and ε_m are the dielectric constant of the surrounding medium / substrate and of the metal, respectively, λ_0 is the monochromatic light source wavelength. This method, while less frequently used in the conventional SPR set-ups, is critical and very efficient where SP excitation on the planar surface by free-space radiation is required and, as is shown in this work, could provide additional parameters for experimental applications.

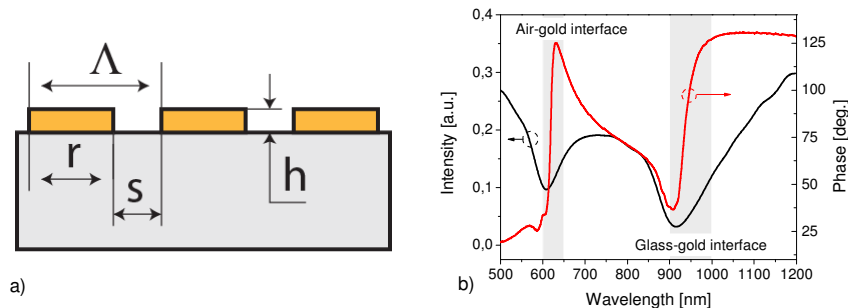


Fig. 1. a) Schematic representation of the nanograting with period d , ridge size r , slit size s and thickness h ; b) Intensity and phase of the light transmitted through the nanoslit array with 600nm period, 450nm ridge size and 100 nm thickness.

While the proposed methodology could be applied to any types of gases or liquids biosensing, we concentrated our effort, as a proof of concept, on gas sensing ($n = 1$) by performing both simulations and experiments on rectangular-slits gratings. The proposed structures (Fig. 1a.) consist of a $h = 100\text{nm}$ thick gold film deposited on a transparent glass substrate (BK7) with a fixed period of $\Lambda = 600\text{nm}$ and a varying ridge size r as an optimization parameter.

As it was shown in the literature [8] the interaction of the incident light with subwavelength metallic structures results in an excitation of normal propagating plasmonic modes and coupled and uncoupled modes that are highly localized resonances. Moreover, these resonances may not propagate between slits, are independent of the grating period and are associated with reflection, extinction and transmission enhancement of the light. Using the rigorous couple wave analysis (RCWA) formalism [9], we performed numerical simulations to obtain the spectral characteristics for phase and intensity of light transmitted through such plasmonic nanostructures. Experimental spectral dependences (Fig. 1b) for an incident light polarization perpendicular to the grating slits contain distinguishing features characterized by a sharp phase jump and a minimum intensity at about 600nm and 900nm attributed to the SP excitations at respectively the air/metal and metal/substrate interfaces. Since sensing occurs at the medium/gold interface, only the spectral range around 600nm is shown later in this work. Figure 2a presents theoretical spectral phase dependences for gratings having a fixed period of $\Lambda = 600\text{nm}$ and varying ridge sizes of $r = 300\text{nm}$, 350nm , 400nm , 450nm and 500nm . Maximising the sensitivity requires to obtain a sharp phase variation around a predetermined working wavelength. As follow from Fig. 2a, the larger is r , the sharper is the phase change. For our system, the optimum condition was achieved for ridge size equal to 450nm at the working wavelength of 632.8nm (He-Ne laser). Here we propose to apply a phase sensing methodology to follow changes of medium refractive index. As an example, after slightly increasing the medium RI by a value equal to 0.003 RIU for sample with $r = 450\text{nm}$, the spectral phase curve is shifting, as shown by the dashed blue line on Fig. 2a. This shift resulted in a corresponding phase change $A \rightarrow B$ at the fixed working wavelength. Dynamic range of the sensor can be estimated from the absolute phase variation ($\Delta\lambda$ on Fig. 2a). It is interesting to point out that the subsequent increase of r to 500nm has rather different impact on phase characteristic, showing opposite spectral trend. Such behaviour is very similar to the surface plasmon phase dependences on the thin metal film thickness in the Kretschmann SPR geometry.

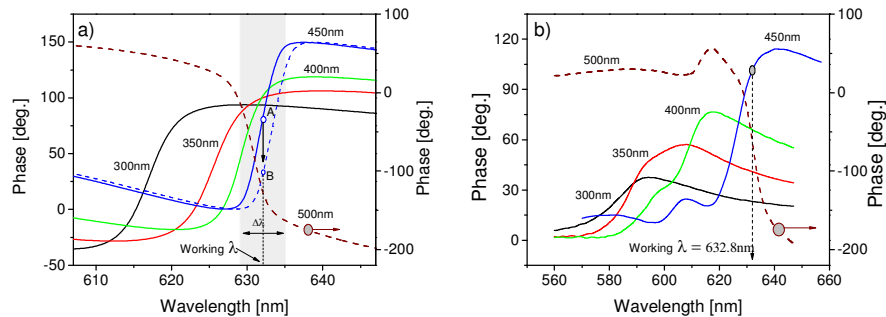


Fig. 2. a) Theoretical spectral phase curves for nanograting structures with different ridge sizes; dashed blue line presents a shifted spectral phase curve for $r = 450\text{nm}$ resulting from a change in refractive index equal to 3×10^{-3} RIU; b) Experimental spectral phase characteristics.

For experimental tests, nanograting arrays with a fixed period of 600nm , ridge sizes ranging from 300nm to 500nm and overall dimension of $150 \times 150 \mu\text{m}$ were produced by Focused Ion Beam (FIB) on a 100nm thick gold metal film (Platypus) deposited on the

transparent substrate (glass BK7). Experimental spectral phase curves were measured on an ellipsometer (J.A. Wollam) and are presented on Fig. 2b. Overall tendencies confirm the theoretical predictions while some differences are observed in spectral phase curves positions and absolute phase variation, which are due to the imperfections of the fabricated samples by FIB method. It is anticipated that surface roughness [10], grating lines and period precision, slight convergence of the probe light could affect the surface waves propagation parameters especially for smaller slit sizes. Additional irregularities presented on the experimental curves are probably due to the complex nature of the light transmission through nanoplasmonic structures [11].

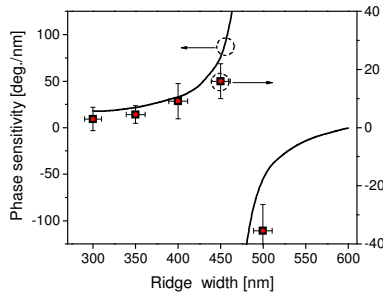


Fig. 3. Theoretical (solid curves; scale on the left) and experimental data (points; scale on the right) for phase sensitivity dependence on the ridge sizes.

Sensitivity and dynamic range of the proposed phase-sensitive method depends on the sharpness and absolute variation of the spectral phase curves (Fig. 2). Usually these sensor parameters are tuned by the plasmon coupling grating period. Here we show how important is the optimization of the ridge sizes and thickness for the nanogratings based sensor. Figure 3 shows the calculated and measured results for sensor phase sensitivity as a function of the ridge width. The obtained lower experimental sensitivity could be improved by performing E-Beam nanofabrication method on larger samples with smoother metal layers.

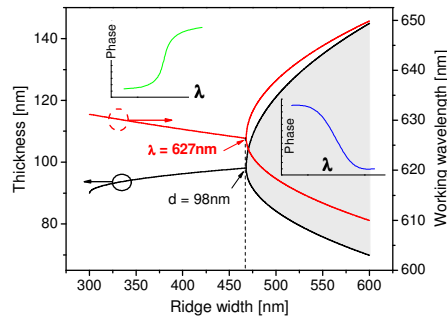


Fig. 4. Theoretical results for optimal grating thickness and corresponding working wavelength position for different ridge sizes; Inserts: Typical phase curves for marked region.

Optimal grating thickness that corresponds to the maximum spectral phase variation was evaluated theoretically for different ridge sizes (Fig. 4. black line). Calculated working wavelengths at the position of the phase maximum are shown as red lines on Fig. 4. It is clear that the minima of transmission and large phase changes follow the SP dispersion line (Eq. (1)). We can apply the concept that the optimal resonance condition of surface plasmon excitation is obtained when internal damping Γ_i is equal to the radiation damping Γ_{rad} [12] and that the direction of phase variation depends on the relation of these two parameters [13].

Radiation damping mechanism in our case contains two components. The first one is backscattering by the grating that increases with the grating thickness. The second is excitation of surface plasmon on the air/gold interface, for which enhanced transmission through nanoslits and coupling to the plasmon on the gold/substrate interface induces reemission to the far field. Γ_i is usually equal to the imaginary part of the propagating surface plasmon wavevector. But, in the case of asymmetrical gratings, the wave which travels parallel to a surface of a medium with a higher refractive index tends to lose energy into that medium and, similarly, the grating lines tend to collect light which initially travels into the grooves. Thus, this effect and the amounts of energy emerging from the grating lines and grooves will affect the internal damping parameter [14]. Using this concept we can explain the behavior of the curve for optimal grating thickness. First, the grating thickness of about 100nm allows compensating Γ_i [15]. Increasing of the ridge sizes results in the increase of Γ_i and requires thicker grating to maintain condition $\Gamma_i = \Gamma_{rad}$. The optimal grating thickness of 98nm is found for ridge width 470nm with a working wavelength of 627nm. This wavelength corresponds exactly to the condition of surface plasmon excitation at gold/air interface on the 600nm grating with normal incidence (Eq. 1). A very interesting effect is observed after this point: splitting of the curve for optimal grating thickness and inversion of the phase curve (Fig. 4, inserts). This effect could be explained by the resonance properties of enhanced light transmission through small subwavelength slits. For example, for nanoslits less than 100nm, different Fabry-Perot modes exist that depend on the slit size and depth [8,16]. Leaking of evanescent surface plasmon also can contribute to the appearance of several optimal thicknesses [11,17]. A deeper, more physical understanding of these phenomena would be desirable, but it takes substantial experimental work and is a subject of a future work.

Due to the nanofabrication technology limitations and the relatively low dynamic range of the phase-sensitive method, coincidence of probing laser light wavelength with the phase curve's maximum slope is rather difficult experimentally. It is critical to find another parameter to tune the starting point, which is generally the maximum phase slope point. To maximise the sensor performance, we opted to tilt the structure. As it could be observed in Fig. 5, angular deviation of the sample enables to tune this point by changing the wavelength position of the maximum phase slope. Therefore, by doing angular measurement at fixed wavelength, it is possible to retrieve the starting point of the experiment.

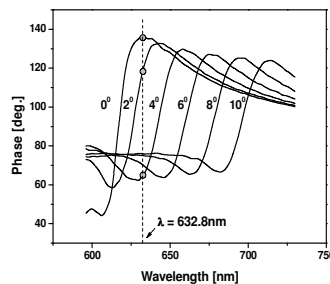


Fig. 5. Experimental phase dependences for different incident angles;

3. Instrumental methodology

An experimental set-up illustrated in Fig. 6 was developed to measure time variations of phase properties in air or liquid medium of our samples. In the proposed polarimetric set-up, spatially filtered light from a 5 mW stabilized He-Ne laser with 632.8 nm wavelength is passed through a Glan-Taylor polarizer to provide a 45° linearly polarized beam. The light is directed to a Photoelastic Modulator (PEM, HINDS I/FS50) after passing through a Soleil - Babinet compensator, which serves to optimize the initial phase retardation. The PEM is used

to sinusoidally modulate the phase of the p-component at a frequency of 50 kHz. The beam is then directed through a diaphragm to the nanoplasmonic structure placed on the high precision rotation stage, thus allowing for incident angle fine tuning. All experiments in air or in gases were performed in a specially designed measurements chamber.

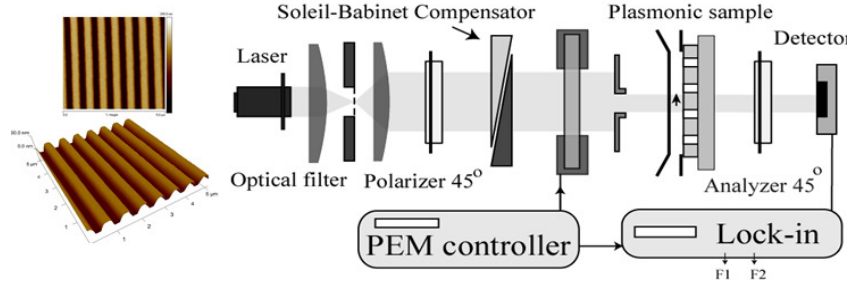


Fig. 6. AFM sample images and optical set-up for phase measurements.

The final periodic signal of light transmitted through the tested nanoplasmonic sample and the 45° oriented analyzer is measured by the detector and then decomposed into harmonics using a lock-in amplifier. Since the time domain signal is periodic and continuous, the harmonics of a frequency spectrum could be modeled using a Fourier transform method. Thus, the first two harmonics are given by [6]:

$$F_1 = 2J_1(M)R_p R_s \sin(\alpha + (\phi_p - \phi_s)) \quad (2)$$

$$F_2 = 2J_2(M)R_p R_s \cos(\alpha + (\phi_p - \phi_s)) \quad (3)$$

Here, α is the initial phase retardance introduced by the Soleil-Babinet compensator. R_p , ϕ_p and R_s , ϕ_s are reflection and phase under p- and s- polarization, respectively. J_n indicates a Bessel function of order n and M, the modulation amplitude. Phase retardation $\phi = \phi_p - \phi_s$ can be derived from Eq. (2) and (3) and are given by:

$$\phi = \tan^{-1} \left(\frac{F_1 J_2(M)}{F_2 J_1(M)} \right) \quad (4)$$

4. Results and discussion

In order to estimate the efficiency of the polarimetric experimental set-up for the proposed nanoplasmonic phase-sensitive methodology, initial calibration tests were performed. In the absence of the sensing block, we measured responses of the first and second harmonic to the small phase retardation introduced by a Soleil-Babinet compensator. Optimal signal-to-noise ratio for the phase measurements (Eq. 4) was obtained at 154° phase modulation depth (M), which provides equal harmonics intensities and therefore optimal conditions for the noise elimination (Fig. 7a). Looking at the noise level, the high phase resolution of $6 \cdot 10^{-3}$ deg. confirms the efficiency of our polarimetric set-up for direct real time phase measurements at fixed incident angle.

To test the proposed methodology, we adapted the PEM-based phase measurement system for nanoplasmonic sensing measurements, as shown in the Fig. 6. Nanoplasmonic samples were placed on the rotation stage and the measured initial phase retardation was compensated by a Soleil-Babinet compensator. Experimental phase-angular dependencies serve as calibration procedure to find the optimal tilt position for highest phase sensitivity. For example, as seen in Fig. 7b, for a nanograting array with ridge = 450nm, the maximum phase derivative is obtained at 2.88 deg. angle tilt which is later fixed for real time gas sensing.

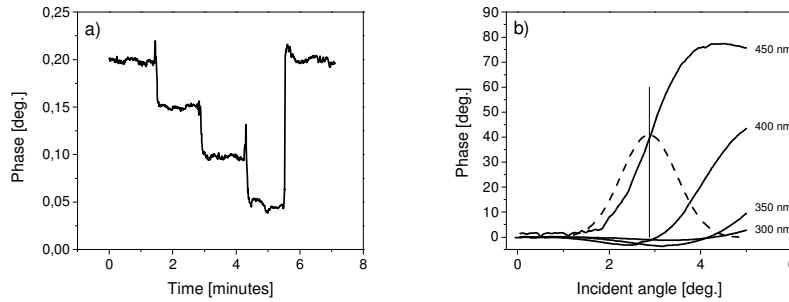


Fig. 7. (a) Phase sensitivity experiment. b) Determination of optimal incident angle.

We then used a well-established gas methodology for small refractive index variations Δn [5]. This method involves comparing the system response, while different inert gases with known refractive indices are brought in contact with the gold film. In the experiments, Ar and N_2 were used, for which the refractive indices differ by $\Delta n \cong 1.5 \cdot 10^{-5}$ RIU under the normal conditions [18, 19]. The gases were brought to the cell through a long spiral copper tube to equilibrate their temperatures with the room temperature. A flow meter is used to equalize the pressure to the flow cell in contact with the SPR-supporting nanoplasmonic gold film. Figure 8 demonstrates typical phase signals under the replacement of pure N_2 by Ar gas. Taking into account the level of residual noises that is equal to 0.06deg. (equal to three times of the mean standard deviation on each step), we can determine that the detection limit of our system is about $3.8 \cdot 10^{-6}$ RIU, which is significantly better compared to conventional spectral-sensitive nanoplasmonic devices. Further improvement of the detection limit could be achieved by optimizing grating parameters, precision of nanofabrication and application of an active thermostabilisation system.

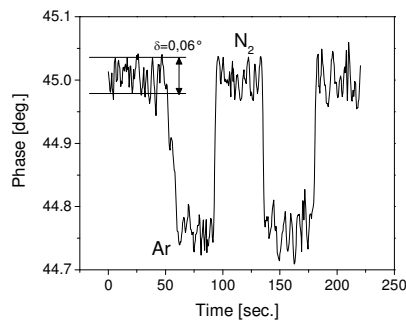


Fig. 8. Experimental results for phase under the replacement of pure N_2 by Ar.

Conclusion

We proposed a dephasing method of SP signal/noise enhancement to improve overall sensitivity of nanoplasmonic structures in bio- and chemical sensing. The proposed method enables to obtain low noise signals with an anticipated resolution of about $3.8 \cdot 10^{-6}$ RIU. Such phase-sensitive approach makes possible the achievement of a relatively low detection limit and is expected to provide substantial advantages in the development of low-cost, portable gas- or biological sensor devices.

Acknowledgment

The authors acknowledge the financial contribution from the NSERC Strategic Network for Bioplasmonic Systems (Biopsys) and NanoQuébec.